Improved laser vibration ladar

Hilaire, Pierre.

Monterey, California. Naval Postgraduate School

NAVAL POSTGRADUATE SCHOOL
Monterey, California

THESIS

IMPROVED LASER VIBRATION LADAR

by

Pierre Hilaire

December, 1998

Thesis Advisor: Robert C. Harney
Co-Advisor Donald L. Walters

Approved for public release; distribution is unlimited.

REPORT DOCUMENTATION PAGE

Form Approved OMB No. 0704-0188

1. AGENCY USE ONLY *(Leave blank)*	2. REPORT DATE December 1998	3. REPORT TYPE AND DATES COVERED Master's Thesis

4. TITLE AND SUBTITLE: IMPROVED LASER VIBRATION LADAR	5. FUNDING NUMBERS
6. AUTHOR(S): Hilaire, Pierre	
7. PERFORMING ORGANIZATION NAME(S) AND ADDRESS(ES) Naval Postgraduate School Monterey, CA 93943-5000	8. PERFORMING ORGANIZATION REPORT NUMBER
9. SPONSORING / MONITORING AGENCY NAME(S) AND ADDRESS(ES)	10. SPONSORING/MONITORING AGENCY REPORT NUMBER

11. SUPPLEMENTARY NOTES The views expressed in this thesis are those of the author and do not reflect the official policy or position of the Department of Defense or the U.S. Government.

12a. DISTRIBUTION / AVAILABILITY STATEMENT	12b. DISTRIBUTION CODE
Approved for public release; distribution is unlimited.	

13. ABSTRACT *(maximum 200 words)*

The Naval Postgraduate School Physics Department is investigating the feasibility of identifying ground combat vehicles by measuring their frequency of vibrations. This thesis reconfigured an existing CO_2 laboratory laser radar system that is capable of measuring the frequencies of vibration of a simulated target into a more compact and rugged form for field testing. The optical performance of the laboratory laser radar system was also improved with a combination half-wave plate, brewster-angle plate, and quarter-wave plate. The new device was tested under laboratory conditions using a target with known frequencies of vibration and a target with a more complex frequency spectrum. Both tests involved illuminating the targets with the laser beam. The first target was a retro-reflector driven by a piezoelectric actuator vibrating at selectable known frequencies (typically 400 Hz). The second target was a 9-volt DC motor supplied with 10 volts and 13 volts respectively in order to vary its speed. The laser radar proved capable of detecting the first target's frequencies of vibrations and the more complex frequency spectrum of the DC motor.

14. SUBJECT TERMS: Laser radar, Half-wave plate, Brewster-angle plate , Quarter-wave plate, Acousto-optic modulator	15. NUMBER OF PAGES 56
	16. PRICE CODE

17.SECURITYCLASSIFI-CATION OF REPORT	18. SECURITY CLASSIFICATION OF THIS PAGE	19. SECURITY CLASSIFI- CATION OF ABSTRACT	20. LIMITATION OF ABSTRACT
Unclassified	Unclassified	Unclassified	UL

Approved for public release; distribution is unlimited

IMPROVED LASER VIBRATION LADAR

Pierre Hilaire
Lieutenant, United States Navy
B.A., Old Dominion University, 1992

Submitted in partial fulfillment of the
requirements for the degree of

MASTER OF SCIENCE IN APPLIED PHYSICS

from the

NAVAL POSTGRADUATE SCHOOL
December 1998

Author: [redacted]
Pierre Hilaire

Approved by: [redacted]
Robert C. Harney, Thesis Advisor

[redacted]
Donald L. Walters, Co-Advisor

[redacted]
William Maier, Chairman
Department of Physics

ABSTRACT

The Naval Postgraduate School Physics Department is investigating the feasibility of identifying ground combat vehicles by measuring their frequency of vibrations. This thesis reconfigured an existing CO_2 laboratory laser radar system that is capable of measuring the frequencies of vibration of a simulated target into a more compact and rugged form for field testing. The optical performance of the laboratory laser radar system was also improved with a combination half-wave plate, brewster-angle plate, and quarter-wave plate. The new device was tested under laboratory conditions using a target with known frequencies of vibration and a target with a more complex frequency spectrum. Both tests involved illuminating the targets with the laser beam. The first target was a retro-reflector driven by a piezoelectric actuator vibrating at selectable known frequencies (typically 400 Hz). The second target was a 9-volt DC motor supplied with 10 volts and 13 volts respectively in order to vary its speed. The laser radar proved capable of detecting the first target's frequencies of vibrations and the more complex frequency spectrum of the DC motor.

TABLE OF CONTENTS

ACKNOWLEDGEMENTS

The author would like to extend special thanks to George Jaksha and Gary Beck, two very fine machinists, for manufacturing the extra parts need for this thesis. Without their help, this thesis would have been much more difficult to complete. A very special thanks to my classmates Scott Bewley, John Holmes, Mark Leary, and Uria Zachary for our long study sessions at the library. Without those guys help, I would never have been able to decipher the professors' coded lectures.

My last gratitude goes to my loving wife Angelia, my two soccer playing sons Josh and Bryant (GO! EAGLES), and the latest addition to our family, my youngest son Nicholas.

I. INTRODUCTION

A. PURPOSE

This thesis is part of continuing research at the Naval Postgraduate School Physics Department to develop a laser radar system capable of identifying a target by measuring its frequency of vibrations. An existing 10-watt, CO_2, laboratory laser radar system can theoretically detect a target's vibrations at ranges of modern ground combat (Day, 1997, p.1). The purposes of this thesis are to reconfigure in a more compact and rugged form this CO_2 laser radar system, to improve its optical performance, and to make it portable for field use.

B. CONCEPTS

"Acoustics involves the generation, transmission, and reception of vibrational energy. The displacement of the atoms or molecules of fluids or solids from their natural configurations produces an internal restoring force. This restoring force and the inertia of a system enable matter to participate in oscillatory vibrations, to generate and to transmit acoustic waves. Most of us have experienced acoustic waves in the form of sound in the 20 to 20,000 Hz frequency range, but acoustics also involve the ultrasonic frequencies above 20,000 Hz and the infrasonic frequencies below 20 Hz". (Sanders, 1982, p.1) The idea of measuring the vibrations of a target to determine its identity is, therefore, conceivable since nearly all mechanical systems vibrate when in operation. In many instances we can tell when they are operating by the characteristic sounds they produce.

The principle of interference and superposition are fundamental in detecting vibrations of military vehicles using laser radar. Detection of a target's vibrations involves the measurement of the relative phase between two electromagnetic waves of

approximately the same frequency and polarization. A reference wave (local oscillator) travels a fixed distance within the laser radar system, while a second wave travels to the target. Upon its return, the second wave is added to the reference wave to produce an interference term, which is a function of the relative phase between the two waves. A nonlinear device such as a mixer or squarelaw detector can isolate the interference term for further processing. The combination of electromagnetic waves is called coherent detection or heterodyne detection. (Day, 1997, p.3)

Figure 1-1 is the offset homodyne configuration, which is used in our system. It uses an acousto-optic device to shift the frequency of the second waver in order to permit the direction of motion to be determined. (Day, 1997, p.4)

II. THEORY

A. MEASURING VIBRATIONS

When two electromagnetic waves overlap at a point in space, the resultant field is equal to the algebraic sum of the fields of the two separate waves. This is known as the principle of superposition. A solution of the differential wave equation can be written as

$$E(\alpha,t) = E_0 \sin(\omega t + \alpha), \tag{2-1}$$

where E_0 is the amplitude of the wave propagating in the positive x direction, and α represents the phase. If we have two such waves

$$E_1 = E_{01} \sin(\omega t + \alpha_1) \qquad \text{and} \qquad E_2 = E_{02} \sin(\omega t + \alpha_2), \tag{2-2}$$

with the same frequency and speed, their overlap at a point in space is a linear superposition of the two waves

$$E = (E_{01}\cos\alpha_1 + E_{02}\cos\alpha_2)\sin\omega t + (E_{01}\sin\alpha_1 + E_{02}\sin\alpha_2)\cos\omega t. \tag{2-3}$$

Because the terms in parentheses are constant in time, we have

$$E_0\cos\alpha = E_{01}\cos\alpha_1 + E_{02}\cos\alpha_2, \tag{2-4}$$

and

$$E_0\sin\alpha = E_{01}\sin\alpha_1 + E_{02}\sin\alpha_2. \tag{2-5}$$

Squaring and adding equations (2-4) and (2-5), we obtain

$$E_0^2 = E_{01}^2 + E_{02}^2 + 2E_{01}E_{02}\cos(\alpha_2 - \alpha_1), \tag{2-6}$$

with an interference term, $2E_{01}E_{02}\cos(\alpha_2-\alpha_1)$. (Hecht, 1987, p.243)

The resultant electromagnetic field derived above varies in time at a very rapid rate of approximately 4 - 8 x 10^{14} Hz, which is impractical to detect directly. The

irradiance, I of the field, however, can be measured using a detector. The irradiance of the field is $I = \langle E^2 \rangle$, which is the time average of the magnitude of the electric field squared, from Equation 2-6

$$I = I_1 + I_2 + 2(I_1 I_2)^{1/2} \cos(\alpha_2 - \alpha_1). \tag{2-7}$$

This indicates that the irradiance is a function of the phase between the two waves via the interference term $2(I_1I_2)^{1/2}\cos(\alpha_2-\alpha_1)$. (Hecht, 1987, p.336)

Our laser radar makes use of the above discussion via the amplitude splitting technique. A reference beam known as a local oscillator travels a fixed distance within the laser radar system to a detector and a second wave travels to the target and back to the detector.

By fixing the distance that the local oscillator beam has to travel, its phase remains constant so we will set $\alpha_1 = 0$. For the second beam, however, there is a direct connection between its phase and the total distance traveled. Taking the distance X ,to the target to be half the round trip distance, we have

$$\alpha_2 = \frac{2\pi}{\lambda} X = \frac{4\pi}{\lambda} x \ . \tag{2-8}$$

For a stationary target at normal incidence, the vibration is assumed sinusoidal with amplitude x_0 and frequency $\omega_t t$. After subtracting the constant large phase $(4\pi x/\lambda)$ due to the average round trip distance to the target, then for a target vibrational displacement of $x = x_0 \sin\omega_t t$, the time dependent phase becomes

$$\alpha_2 = \frac{4\pi}{\lambda} x_0 \sin \omega_t t, \tag{2-9}$$

and the total irradiance

$$I = I_1 + I_2 + 2(I_1 I_2)^{1/2} \cos(\frac{4\pi}{\lambda} x_0 \sin \omega_t t) .$$ (Day, 1997, p.8) (2-10)

1. Target Beam Frequency Shift

The interference term in the irradiance oscillates at the target's frequency of vibration. However, a problem remains. Motion of the target toward and away from the detector produces the same change in phase. Shifting the second beam by a frequency ω_s corrects this problem. This causes the phase of the second beam to become

$$\alpha_2 = \omega_s t + \frac{4\pi}{\lambda} x_0 \sin \omega_t t . \quad (2\text{-}11)$$

The irradiance then becomes

$$I = I_1 + I_2 + 2(I_1 I_2)^{1/2} \cos(\omega_s t + \frac{4\pi}{\lambda} x_0 \sin \omega_t t) . \quad (2\text{-}12)$$

Changes in irradiance will vary around the frequency ω_s provided that $\omega_s t \geq \frac{4\pi}{\lambda} x_0 \sin \omega_t t$. Any net translational velocity also effects the target beam's frequency. It causes a Doppler shift to the frequency. For a target moving with net velocity υ, the frequency of the target changes by

$$f_m = \frac{2\upsilon}{\lambda} \cos\theta . \quad (2\text{-}13)$$

(Day, 1997, p.9) Figure 2-1 shows the various shifts to the target beam's frequency as the beam travels from the laser to the detector.

Errors in measuring the vibrations of the target may result if the combined effects of the Doppler and vibrational frequency shifts are not taken into account. The Doppler shift of a fast moving target can exceed the offset frequency ω_s. Doppler shifts of up to 26 MHz may occur for a 10.6μm wavelength laser for a velocity of 1.8×10^3 $m.s^{-1}$. The

Naval Postgraduate School's laser uses an acouto-optic modulator (AOM) to shift the second beam's frequency. The AOM selected can provide a frequency shift of up to 30 MHz, accommodating almost all subsonic targets. (Day, 1997, pp.9-10)

2. Coherence, Coincidence, and Parallelism

For effective interference while superimposing the two beams at the detector, it is important that the waves are coherent. This will ensure that changes in the phase of the beams are due solely to target motion and vibration (Day, 1997, p.11). Coherence occurs when the temporal and spatial variations of the electric field of the two waves are identical. Spatial coherence is a measure of the autocorrelation length of the field tranverse to the direction of propagation. Temporal coherence is a measure of the autocorrelation length of the wave. (Wilson, 1989, p.233) Lasers are ideally suited as sources for coherent beams.

Two other factors for effective interference are coincidence and parallelism of the two beams at the detector. Figure 2-2 is an illustration of two beams on a detector surface. For two beams of the same wavelength with a small angle β between them, constructive interference occurs in the plane marked (++++), while destructive interference takes place in the plane marked (.....). The distance S, between the interference fringes varies according to changes in the relative phase of the beams. As the fringes move across the detector, a given point on the detector surface will experience fluctuations in irradiance. Fluctuations in irradiance will tend to cancel each other for fringe spacing less than twice the beam diameter. The fringe distance is derived from the following equation

$$S = \frac{\lambda}{2\sin(\frac{1}{2}\beta)} \approx \frac{\lambda}{\beta}. \tag{2-14}$$

For full efficiency η_h, the beam width D_b , must be less than half the fringe spacing S. The two beams must be parallel to within

$$\beta = \frac{\lambda}{2D_b}. \tag{2-15}$$

For a beam width of 1mm, the maximum angle between the two beams for our system was 5.3 mrads. (Day, 1997, pp.12-13)

B. LASER RANGE EQUATION

The beam transmitted by the laser radar and the beam received by the detector can vary significantly. The beam is affected by the components of the laser radar system and other factors such as atmospheric turbulence and attenuation. To understand how the beam is effected as it travels to and from the target, the use of the laser radar range equation is necessary. The equation expresses the signal to noise ratio in terms of how much of the transmitted signal is recognizable from the noise encountered to and from the target. The laser radar range equation for a diffuse-reflectance circular disk and for a TEM_{00} laser mode is (Harney, 1993):

$$SNR = \frac{\eta_D \in_T \in_R P_T e^{-2\alpha R}}{hfB}(\frac{\rho w_0^2}{R^2})[1 - e^{(\frac{-4\pi w_0^2 r_T^2}{\lambda^2 R^2})}], \tag{2-16}$$

η_D is the detector quantum efficiency, $\in_T(\in_R)$ is the transmit(receive) path optics transmission coefficients, w_0 is the guassian spot size at the transmitting aperture of the laser radar, α is the atmospheric attenuation coefficient, ρ is the target reflectivity, r_T is the target radius of an assumed circular target, λ is the wavelength of the beam, R is the

range to the target, f is the frequency of the beam, h is Planck's constant , and B is the electronic bandwidth. There are two limiting cases of the laser range equation.

1. Short Range Resolved Target Limit

At short ranges, $R << 2\pi w_0 r_t/\lambda$, the term produced by the exponential is much smaller compared to 1 and can be neglected to yield a different form of the laser range equation for short range resolved target limit as (Harney, 1993):

$$SNR = \frac{\eta_D \in_T \in_R P_T e^{-2\alpha R}}{hfB}\left(\frac{\rho w_0^2}{R^2}\right). \quad (2\text{-}17)$$

2. Long Range Unresolved Target Limit

At long ranges, $R >> 2\pi w_o/\lambda$, the term produced by the exponential can not be neglected. Expanding the exponential term yields (Harney, 1993):

$$SNR = \frac{\eta_D \in_T \in_R P_T e^{-2\alpha R}}{hfB}\left(\frac{4\pi^2 \rho r_T^2 w_0^4}{\lambda^2 R^4}\right). \quad (2\text{-}18)$$

A relationship exists between the optics of the system and the Guassian spot size w_o. The diameter D, of the optics is selected so that maximum intensity of the Guassian beam profile passes through the optics. This relationship can be expressed as $D = \sqrt{M} w_o$, where M is the optics beam waist matching factor. Acceptable values of M range from 4 to 8, with M = 5 being probably optimum in the trade between increased energy transmission (increased M results in reduced truncation of the edges of the beam) and decreased beam width (increased M results in smaller w_o for fixed D, increased beam divergence, and reduced intensity at the target). (Harney, 1993).

III. IMPROVED LASER RADAR CONSTRUCTION

At the beginning of chapter one, the purpose of this thesis involved the reconfiguration of an existing 10 watt, CO_2, laboratory laser radar system to a more compact and rugged form. It also involved modifying the optical performance and making the laboratory laser radar portable for field use. This chapter describes the modifications to the existing laboratory laser radar.

A. LABORATORY LASER RADAR

The 10 watt, CO_2 laboratory laser radar was built by Captain James V. Day, U. S. Army, as a part of his thesis research while he was a student at the Naval Postgraduate School. For greater details about the construction of the laboratory laser radar, the interested reader is directed to Day's thesis (Day, 1997, pp.39-60).

1. Original Set-up

Figure 3-1 shows the layout of the laboratory laser radar. The lenses, mirrors, and beam splitters were 25 mm in diameter and mounted on Melles Griot gimbal mounts. The mounts allowed adjustments about the vertical and horizontal axes. The mounts were installed on posts fitted to an Edmund Scientific post and rail system. The system used two sets of rails. The first beam splitter after the laser, the acousto-optic modulator, beam splitter, and beam expander were mounted to the first rail. The second rail contained the local oscillator tuning mirror, recombination beam splitter, and the detector. All of theses were then fixed to an optical breadboard. The optical breadboard was a TMC series 78 and was 2 feet by 5 feet and four inches thick. The target was mounted separately from these components. (Day, 1997, pp.44-45)

B. COMPONENTS OF IMPROVED LASER RADAR SYSTEM

Figure 3-2 shows the layout of the improved laser radar system. Most of the components used were part of the laboratory laser radar system. The additional components included two mirrors, a half-wave plate, a brewster-angle plate, and a quarter-wave plate. Mirrors 1 and 2 were used strictly to redirect the laser beam. The half-wave plate, brewster-angle plate, and quarter-wave plate were introduced to improve the optical performance of the laboratory laser radar system. These components increased the amount of the signal returned by the target for interference with the local oscillator. Not all the components illustrated in Figure 3-2 are discussed below. In addition to the components used to improve the optical performance of the laser radar, only the laser, the acousto-optic modulator, and target are discussed.

1. CO_2 laser

The laser used in our system is a Synrad Model G48-1-28, 10.6 μm, CO_2 laser rated at 10 watts. It is powered using a HP-6038A power supply to provide the required 28 volts DC for the laser. The lasing action of the laser is controlled by a HP-6216A power supply. The HP-6216A provided 5 volt "TTL" control voltage that also activated a safety circuit to allow five seconds before the laser began to lase. The laser was air cooled while being used in the laboratory configuration, however, in the new configuration, the laser is not provided with any cooling. Cooling was deemed unnecessary at this point in the development process because the system was never operated long enough for overheating to occur, although the thermal expansion did cause longitudinal mode changes. In case of overheating, the laser contained an internal thermal protection device. Air cooling can be easily reintroduced at a later date if deemed

necessary. More details on laser operation can be found in Day's thesis or the manufacturer's operation manual. (Day, 1997, pp.42-45)

2. Acousto-Optic Modulator

The acousto-optic modulator is from the IntraAction Corporation (Model AGM-406B1). The RF power supply used to drive the modulator is GE model 3030. It is rated at 30 watts and 30 MHz. In order to properly shift the frequency of the oncoming laser beam, the acousto-optic modulator must be oriented at the Bragg angle in relation to the beam. This was accomplished by mounting the modulator on a Newport dual-axis rotational stage. The Bragg angle of 28.91 mrads was achieved by following the procedures used by Day in his thesis. This involved setting the RF driver at maximum power and adjusting the angle of the modulator while watching the two beams on special IR beam probes. At the Bragg angle, the shifted beam is much stronger in intensity than the unshifted beam. The unshifted beam is blocked with the half-wave plate mount. The acousto-optic modulator must be oriented in the vertical position for maximum efficiency in shifting the laser beam. This is because this efficiency is achievable only when the base of the modulator is parallel to the polarization of the beam.

The acousto-optic modulator is water cooled by a small variable speed pump. This allows the delivery of up to the four gallons of water required to adequately cool the modulator. Figure 3-3 is an illustration of the modulator disposition in the laser radar system.

3. Half-Wave Plate, Brewster-Angle Plate, and Quarter-Wave Plate

A light beam that is incident on a surface is illustrated in Figure 3-4. When the beam's polarization vector is perpendicular to the plane of incident, it is reflected in comparison to a light beam with its polarization vector parallel to the plane of incidence. The amount of light that is reflected will vary according to the angle of incidence. For an angle $\theta = \theta_B$ called the Brewster angle, all of the parallel beam will be transmitted, while all of the perpendicular beam will be reflected. (Wilson, 1989, pp.7-8)

The brewster-angle plate with the half-wave plate and quarter-wave plate replaced the beam splitter between the acousto-optic modulator and the beam expander in the laboratory laser radar system. In the laboratory laser radar system, not all of the backward traveling beam from the target was reflected toward the recombination beam splitter. Some of the beam was transmitted through the beam splitter and lost as part of the returning signal. This may not be a problem in the laboratory, however, it can be a problem in the field where the returning signal would be small. The brewster-angle plate along with the half-wave plate and quarter-wave plate reflected the backward traveling beam toward the recombination beam splitter for interference with the local oscillator, therefore, improving the optical performance of the system.

The beam coming from the laser was polarized in the horizontal plane. The half-wave plate was installed with its optical axis at 45 degrees to the laser beam. It polarized the beam in the vertical direction for transmission through the brewster-angle plate. The beam now encountered the quarter-wave plate, which was also installed with its optical axis at 45 degrees. The quarter-wave plate circularly polarized the beam. The beam remained circularly polarized after reflection from the target. The second pass through

quarter-wave plate then horizontally polarized it. The beam is essentially rendered perpendicular to the plane of incidence at the brewster-angle plate. Since the brewster-angle plate was oriented at the brewster angle, $\theta_B = 67.7$ degrees, the backward traveling beam was totally reflected toward the recombination beam splitter across from the brewster-angle plate. This entire process is illustrated in Figure 3-5.

C. SUPERIMPOSING THE TWO BEAMS

In chapter one, it was mentioned that the superposition of the local oscillator and target beam was a necessary condition in measuring the vibrations of the target. This process was performed at the recombination beam splitter.

The recombination beam splitter was positioned to receive the reflected beam at its center. This was accomplished by manual adjusting the position of the beam splitter and then verifying that the beam was on-center using CO_2 beam probes. The reference beam was superimposed onto the target beam using the tuning mirror immediately before the recombination beam splitter. The process was accomplished using the CO_2 beam probe to observed the reference beam moving onto the target beam. Figure 3-6 illustrates this. The surface of the beam probe must be illuminated by ultra violet light and the beam appears as a dark spot on the surface of the probe. The resultant beam is directed toward the detector via the angular adjustments available on the beam splitter, again using the CO_2 beam probe to observe the resultant beam. Final adjustment for the resultant beam on the detector surface was accomplished by moving the detector itself. The detector mount can be adjusted up or down, fore and aft, or laterally.

D. COMPACTNESS AND RUGGEDNESS

The components of the improved laser radar were mounted on a TMC optical breadboard, 3 feet by 1 foot and 2 inches thick. The surface of the breadboard was perforated with 1/4-20 threaded holes. The holes were located one inch apart when measured center-to-center. This provided an accurate way to position the components and to achieve the desired compactness.

All mirrors, lenses, and beam splitters were mounted on 4 in by 1 in and .375 in thick plates. These plates were stacked three high as depicted in Figure 3-7. The face of the plates contained a continuous slot that permitted lateral or fore and aft movement of the lenses during alignment. The plates were attached to the breadboard using two one and half-inch long machine screws. The three plates were used instead of a solid mount because the plates were available in plentiful amounts and when stacked three high, they were the exact height necessary for lens and laser beam intersection.

In addition to the three plates, an additional spacer of ¼ in thickness was used as part of the mounts for the second mirror after the laser and the beam splitter prior to the acousto-optic modulator. This enabled the shifted beam to exit the modulator in a horizontal direction. The reason is explained using Figures 3-8a and 3-8b. In Figure 3-8a, the laser beam enters the acousto-optic modulator from a horizontal direction. The shifted beam exits in a direction away from the horizontal, while the unshifted beam exits horizontally. Figure 3-8b shows the laser beam entering the modulator at an angle equal to the Bragg angle. The shifted beam exits horizontally, which is ideal for the alignment of the optical components in relation to the exiting laser beam.

E. TARGET SIMULATION

The improved laser radar system was tested under laboratory conditions using a small corner cube target with a known vibrational frequency and a target with a more complex frequency spectrum. This target is described in chapter four.

A piezoelectric actuator was used to drive a retro-reflector as depicted in Figure 3-9. The actuator was a Thor Labs Model PE-4 and was capable of displacements of 17.4 μm when driven by a sinusoidal voltage of 0-150 volts. The retro-reflector was from Edmund Scientific. The entire target and retro-reflector assembly were mounted separately from the laser radar system. A signal generator provided the sinusoidal voltage and frequency. This signal was amplified using a Thor Labs amplifier model MDT 691 prior to connection to the piezoelectric actuator. More details about the target and the piezoelectric actuator can be found in Day's thesis. (Day, 1997, pp.52-57)

F. LASER RADAR ELECTRONICS

The electronics used in the improved laser radar were the same as used in the laboratory laser radar. The electronics converted the resultant of the superimposed beams at the detector to a current signal that can be processed by a signal analyzer. The detector was a Belov Technology HgCdTe detector Model B10R-40. This is a room temperature detector, which eliminates the need for cryogenics at the expense of sensitivity. A transimpedance amplifier from Melles Griot amplified the current signal in the detector. The transimpedance amplifier also produced the necessary biasing for the detector.

A series of mini-circuits high pass, low pass, and band pass filters were used in conjunction with a Miteq limiter to restrict the frequency range, to improve system performance, and to stabilize fluctuations in signal amplitude. The system provided a

frequency range centered on 30 MHz with a bandwidth of 20.9 MHz. The signal from the filters and Miteq limiter was applied to a Miteq frequency discriminator. The discriminator was used to convert frequency modulation in the signal into amplitude modulation. (Day, 1997, pp.57-59) The electronics configuration is provided in Figure 3-10.

G. SAFETY

The improved laser radar was constructed and tested in a laboratory room certified for class IV standards by the Naval Postgraduate School Radiation Safety Officer. Safety procedures and standards used during the construction of the laboratory laser radar directly applied in the construction of the improved laser radar. The necessary safety procedures and standards were taken from chapter III and the appendix of Day's thesis.

IV. IMPROVED LASER RADAR TESTING AND EVALUATION

The testing of the improved laser radar involved the use of a retro-reflector target of known vibrational frequency and a target with a complex frequency spectrum. The signal resulting from the interaction of the laser beam and the vibrating target was analyzed using a Wavetek high pass filter (Model 753A) and a HP-3561A digital signal analyzer. The Wavetek high pass filter was connected between the output of the electronics and the signal analyzer. The Wavetek high pass filter was set at high pass cutoff of 20 Hz and a gain of +20 dB. The signal analyzer was on AC couple.

A. IDENTIFYING TARGET VIBRATIONAL FREQUENCIES

1. Target with known Frequencies of Vibration

In our first tests of the improved laser radar, target vibrational frequencies of 400 and 500 Hz were used. Figure 4.1 is an illustration of the target's frequency at 400 Hz with no averaging. The 400Hz and 500 Hz frequencies were detected by the laser radar system and are illustrated in figure 4-2 and 4-3. Figure 4-2 shows the 400 Hz signal at –54.76 dBV and figure 4-3 shows the 500 Hz signal at –61.31 dBV. Target amplitude for both frequencies was set at 1.74μm. The target spectra was averaged to enhance the signal to noise ratio. It is clear that averaging the signal does make it easier to identify the target's frequency of vibration.

During the testing, we experienced nearly continuous fluctuations in the magnitude of the display from the signal analyzer and the appearance of a few other frequencies. The fluctuations caused the magnitudes of the frequencies shown on the display to rise and then fall. Figure 4.3 shows the 400 Hz signal at –37.04 as a result of

fluctuations. The source of the fluctuations was not positively identified but they appeared with a characteristic time constant measured in seconds. The fluctuations may have been the result of thermal expansion of the laser cavity and changes in the longitudinal mode structure since our laser was not cooled during testing. We were able to exclude most unwanted frequencies from the signal during testing through the use of the Wavetek high pass filter and by AC couple the signal analyzer, however, we still experienced some unwanted frequencies. These frequencies were more prominent at 120Hz, 160hz, and 200 Hz and are illustrated in Figure 4-4. We were unable to identify the source of these frequencies. They may be frequencies carried on the electrical power in the laboratory. They may also be building vibrations produced by machines elsewhere in the building.

2. Target with more Complex Frequency Spectrum

Our tests included not only a target with known sinusoidal frequencies of vibration but also a target with a more complex frequency spectrum. We were able to conduct this test by making a simple modification to the existing target configuration. We removed the piezoelectric actuator and mounted a 9 volt DC motor in its place. The retro-reflector was attached to the casing of the DC motor. Power to the DC motor was supplied via a HP triple output power supply (Model 6236B). We successfully detected the frequency spectrum produced by the rotating DC motor.

In order to ensure that we indeed detected the more complex frequency spectrum of the rotating DC motor, we varied the voltage supplied to the DC motor to change its speed. Figure 4.5 shows the frequency spectrum for a frequency span of 1000 Hz and DC motor supplied voltage of 10 volts and figure 4-6 is the frequency spectrum for 13 volts

DC motor supplied voltage. Notice the change in the frequency spectrum for the two different DC motor speeds. We also expanded the frequency span to 2000 Hz and examined the frequency spectrum at the two DC motor supplied voltages of 10 volts and 13 volts. Again notice the change in the frequency spectrum for the different motor speeds and the tapering off of the signal at the higher frequencies as illustrated by Figures 4-7 and 4-8. We conducted a simple experiment to see if the tapering off of the spectrum was indeed occurring and it was not due to a lack of sensitivity of the laser radar to detect the higher frequencies.

In the experiment, we collected data on the piezoelectric driven target for an applied voltage of 18 volts and sinusoidal displacement of 8μm. Figure 4-9 illustrates the result of the experiment. The curve in Figure 4-9 is a transfer function for the sinusoidal displacement. In Figure 4-9, we see that as frequency increased, the signal magnitude decreased indicating a decrease in target displacement. The decrease in magnitude was constant except from 225 Hz to 375 Hz where we saw the resonant frequencies of the retro-reflector and piezoelectric actuator.

Based on the results of the experiment as depicted in Figure 4-9, we concluded that the more complex frequency spectrum of the DC motor was tapering off at the higher frequencies. We also concluded that the results illustrated in Figures 4-5, 4-6, 4-7, and 4-8 were caused by the rotation of the DC motor and not by noise introduced into the system.

B. CONCLUSIONS

The Naval Postgraduate School Physics Department now has an improved laser radar system for continued research on target identification based on frequencies of

vibration. This thesis took an existing laboratory laser radar system and made it more compact and rugged. It also improved the optical performance of the laboratory laser radar system through the use of a combination half-wave plate, brewster-angle plate, and quarter-wave plate. The improved laser radar system successfully detected the frequencies of vibration of a simulated target with known frequencies of vibration and the more complex frequency spectrum of a vibrating electric motor.

The improved laser radar system in its present form will require further modifications to be fully portable for field use and the source of the laser radar changes in detected amplitude must be determined or verified. The changes in detected amplitude probably arise from thermal expansion of the laser cavity. Recommendation is to cool the laser and see if they go away. The modifications should be simple to accomplish. One of the modifications calls for mounting the optical section of the system on a tripod. Since the breadboard upon which the optical components are mounted is perforated with 1/4-20 threated holes on both sides, all that will be required is to bolt the breadboard to the tripod. The next modification involves the auxiliary components of the laser radar system. The auxiliary components consist of the cooling pump and water supply for the acousto-optic modulator, 30 MHz RF driver, laser power supply, and the electronics. The auxiliary components will be installed on a mobile cart. The cart will be constructed with large wheels to facilitate movement on poor surfaces. Once these modifications are carried out, immediate field testing of the improved laser radar can commence.

FIGURES

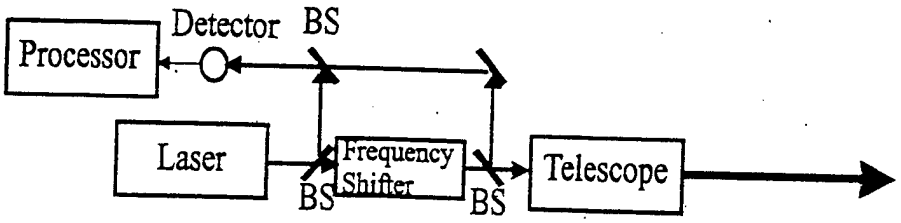

Figure 1-1. Offset Homodyne Detection Configuration. (Day, 1997)

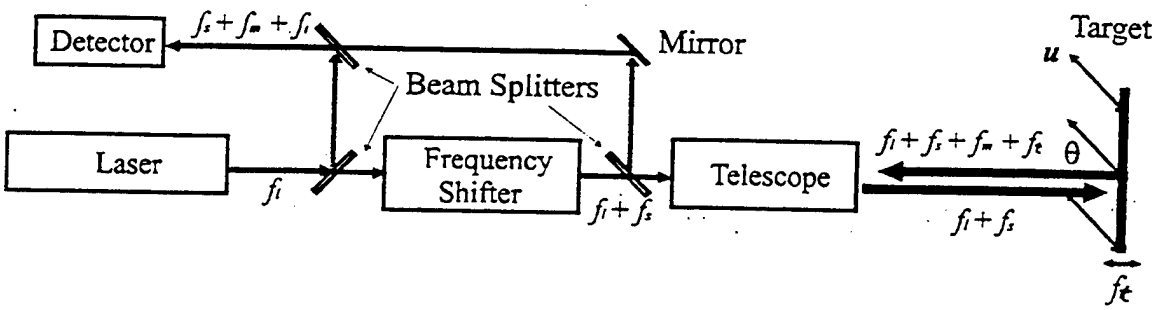

Figure 2-1. Various Shifts of the Target Beam's Frequency. f_l is the Laser Frequency, f_s is the Modulator Frequency, f_m is Doppler Frequency due to Target Motion, and f_t is Target Vibration Frequency. (Day, 1997)

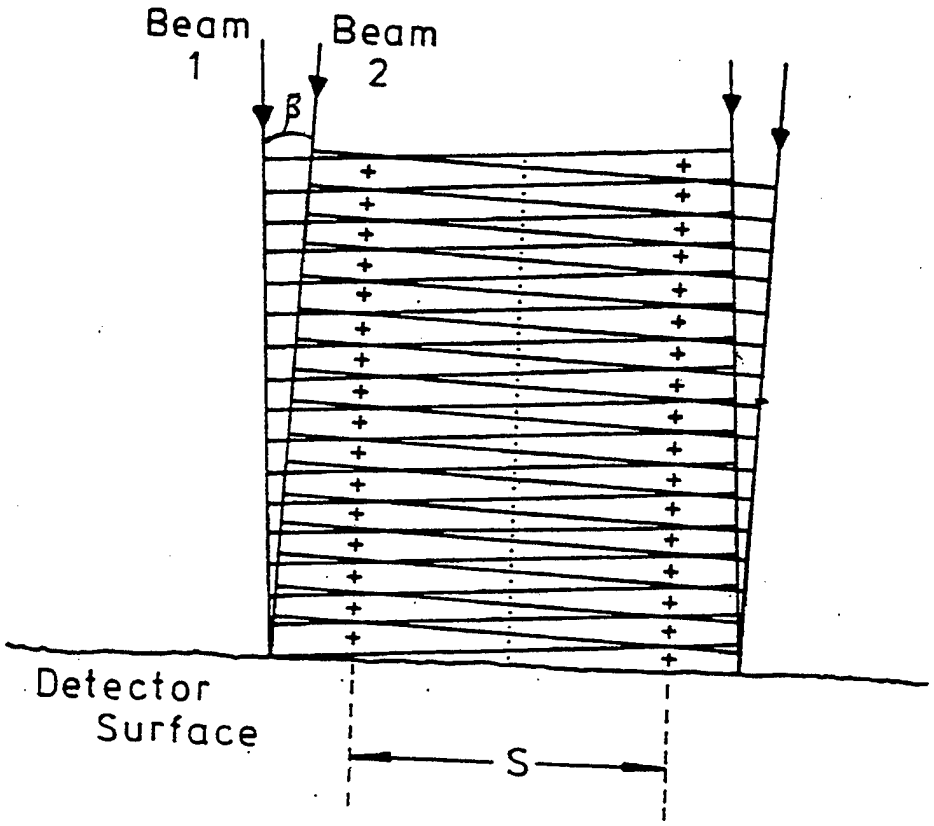

Figure 2-2. Coincidence and Parallelism of two Beams on a Detector Surface. (Day, 1997)

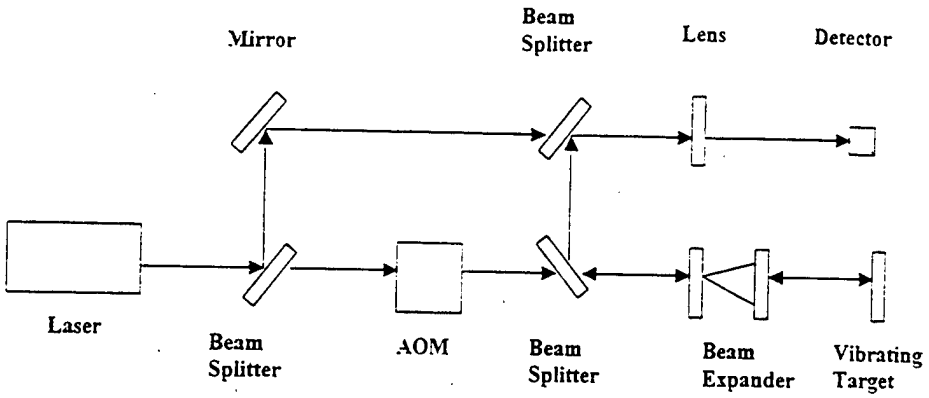

Figure 3-1. Laboratory Laser Radar Layout

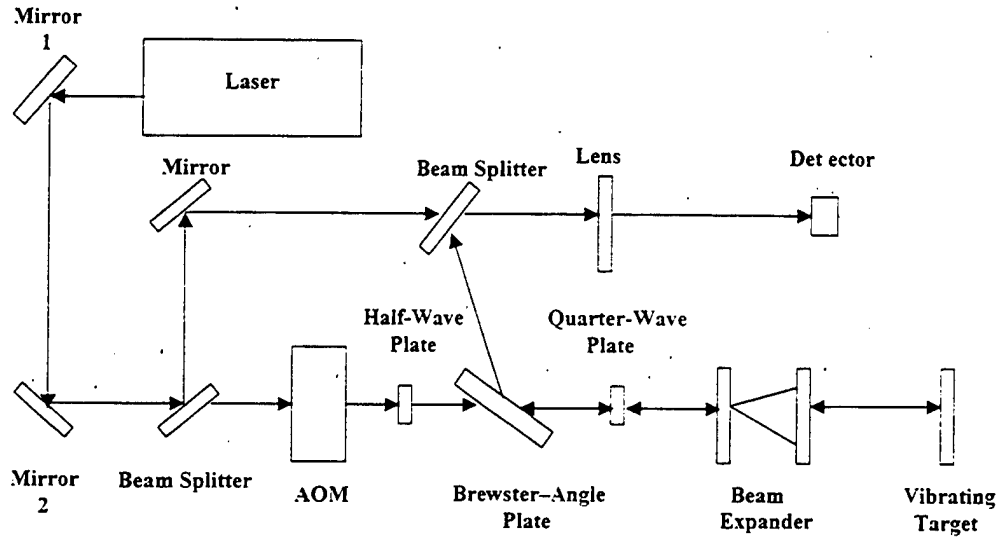

Figure 3-2. Improved Laser Radar layout

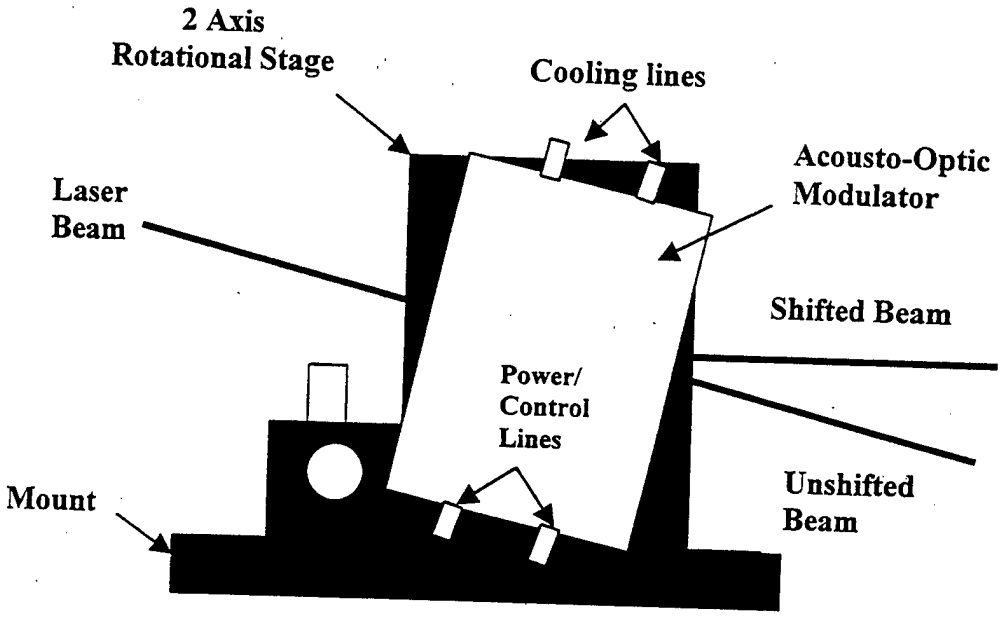

Figure 3-3. Acousto-Optic Modulator Set-up

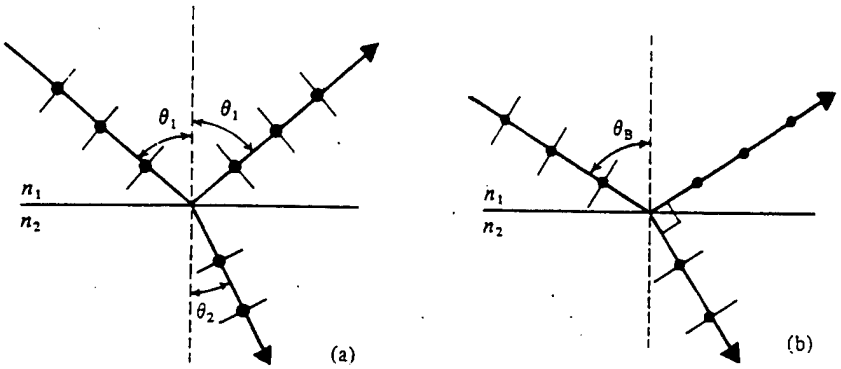

Figure 3-4. (a) Partially Plane Polarized Light Reflected from Interface and (b) Completely Plane Polarized Reflected Light for Incidence at Brewster Angle. (Wilson, 1989)

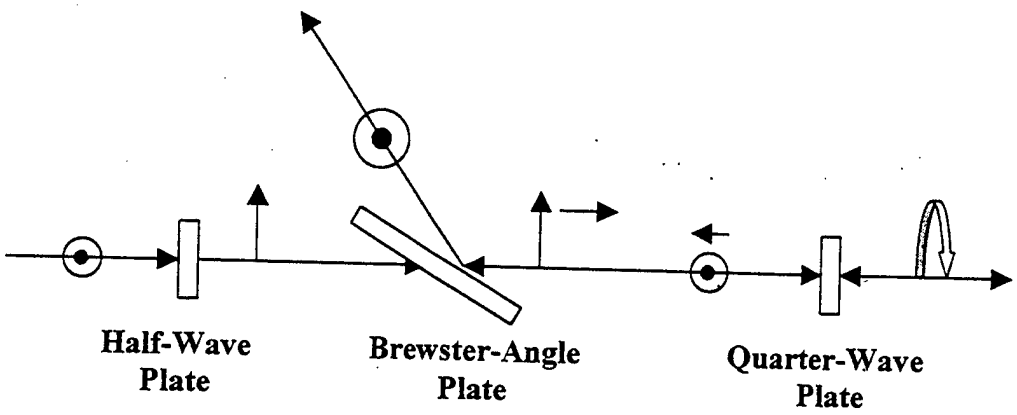

Figure 3-5. Effects of Half-Wave Plate, Brewster-Angle Plate, and Quarter-Wave Plate on Beam Polarization.

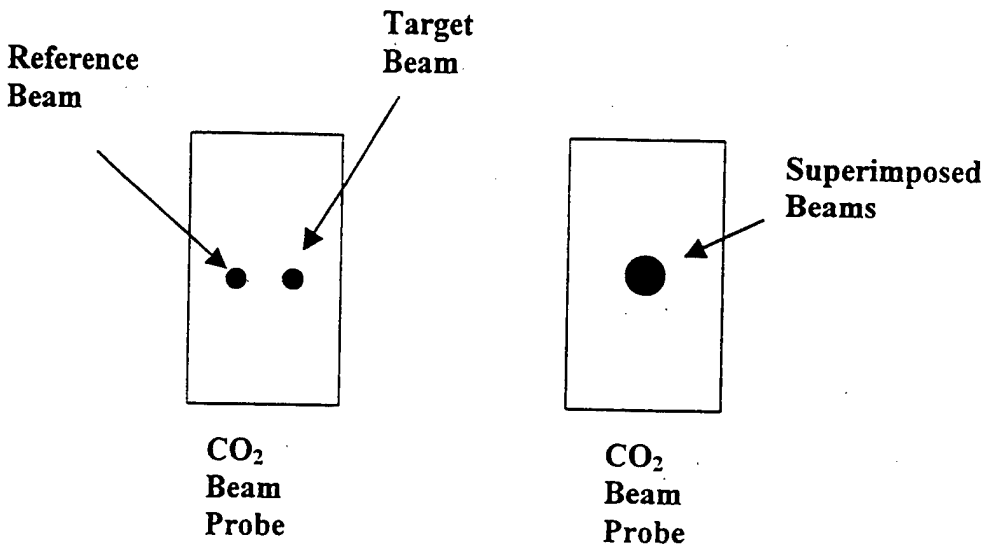

Figure 3-6. View of Reference and Target Beams on CO_2 Beam Probe before and after Superposition.

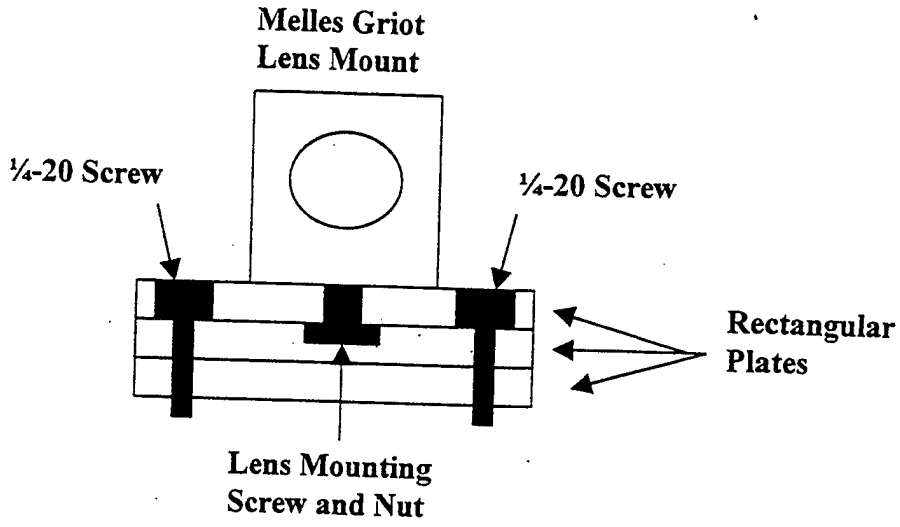

Figure 3-7. Mounting of Optical Components to Breadboard.

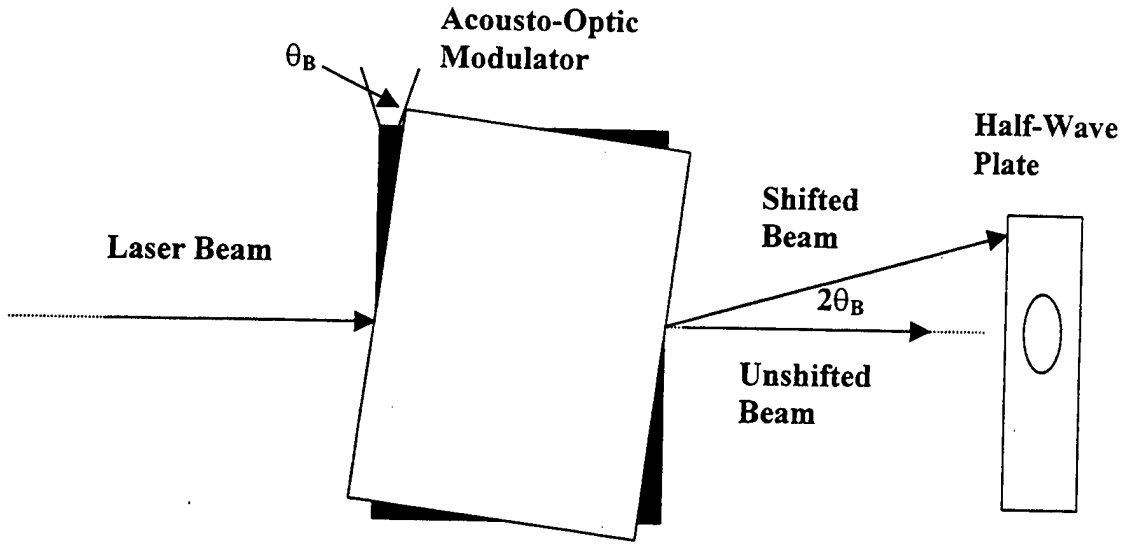

Figure 3-8a. Acousto-Optic Modulator Configuration for Normal Incidence of Laser Beam.

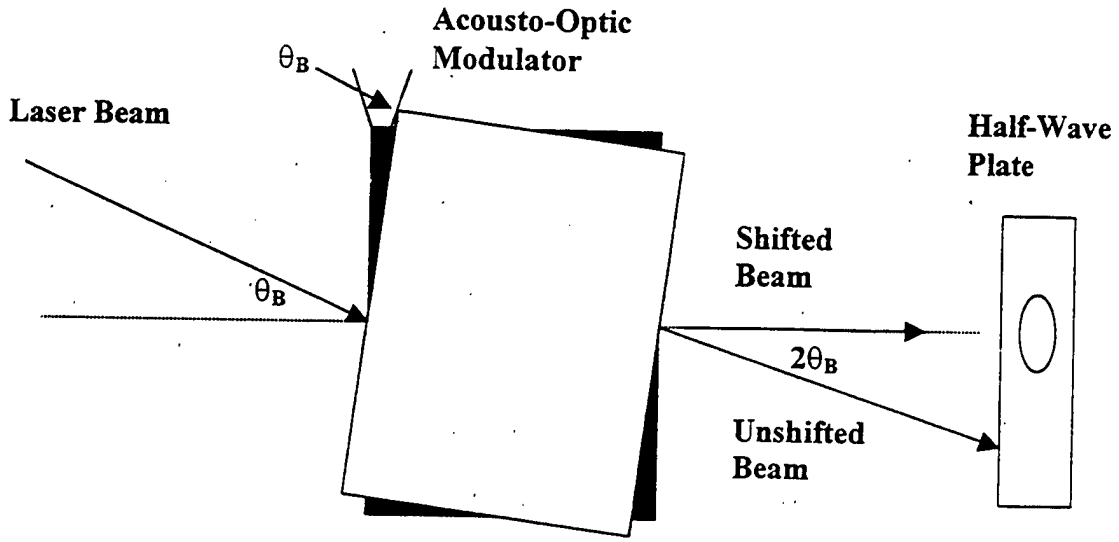

Figure 3-8b. Acousto-Optic Modulator Configuration for Incidence at Bragg Angle.

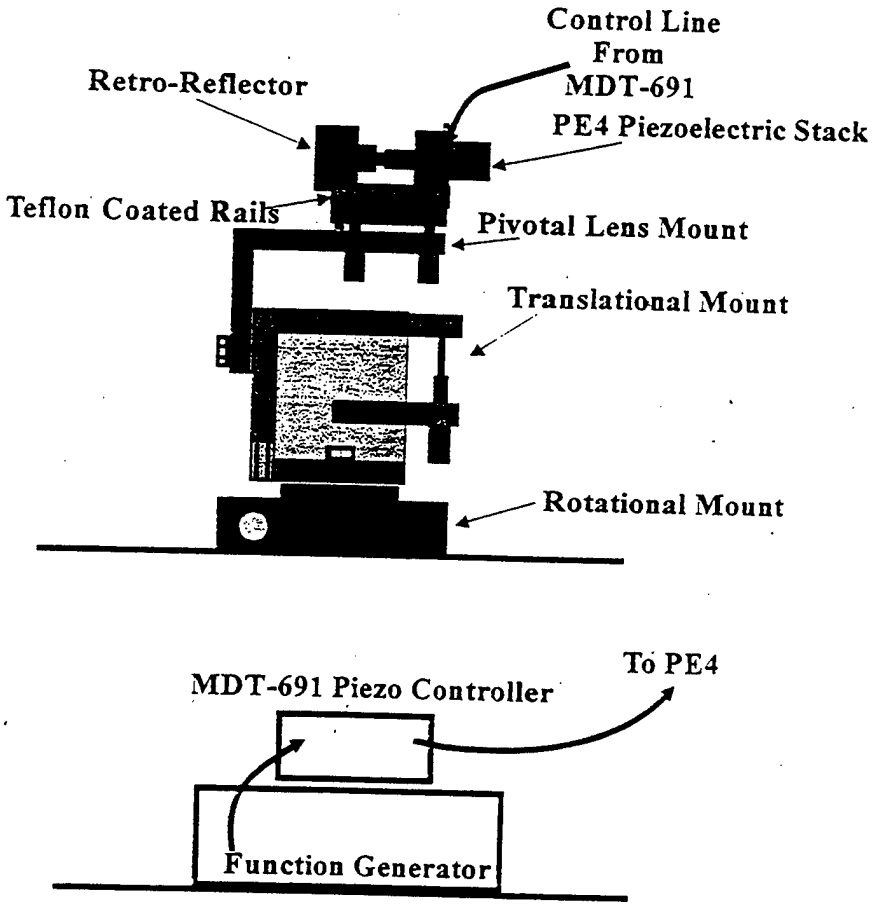

Figure 3-9. Simulated Target Configuration. (Day, 1997)

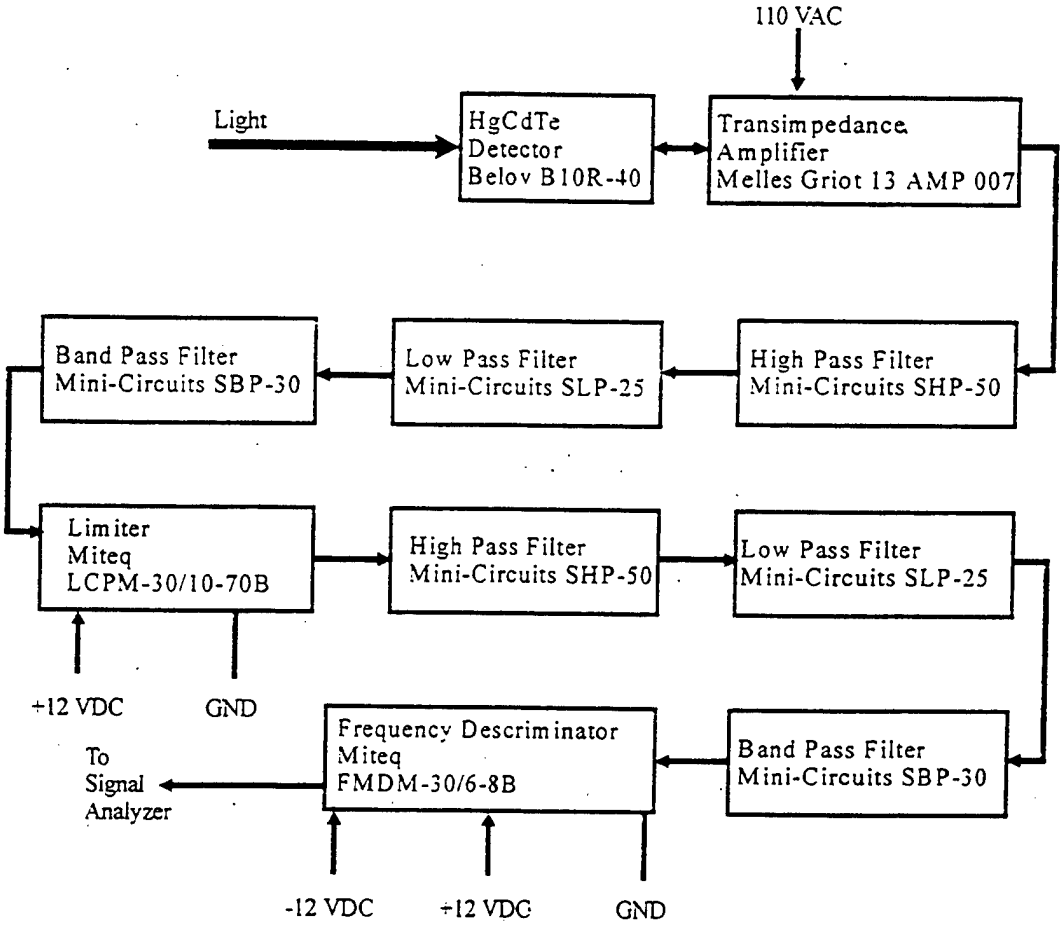

Figure 3-10. Block Diagram of Electronics Circuits. (Day, 1997)

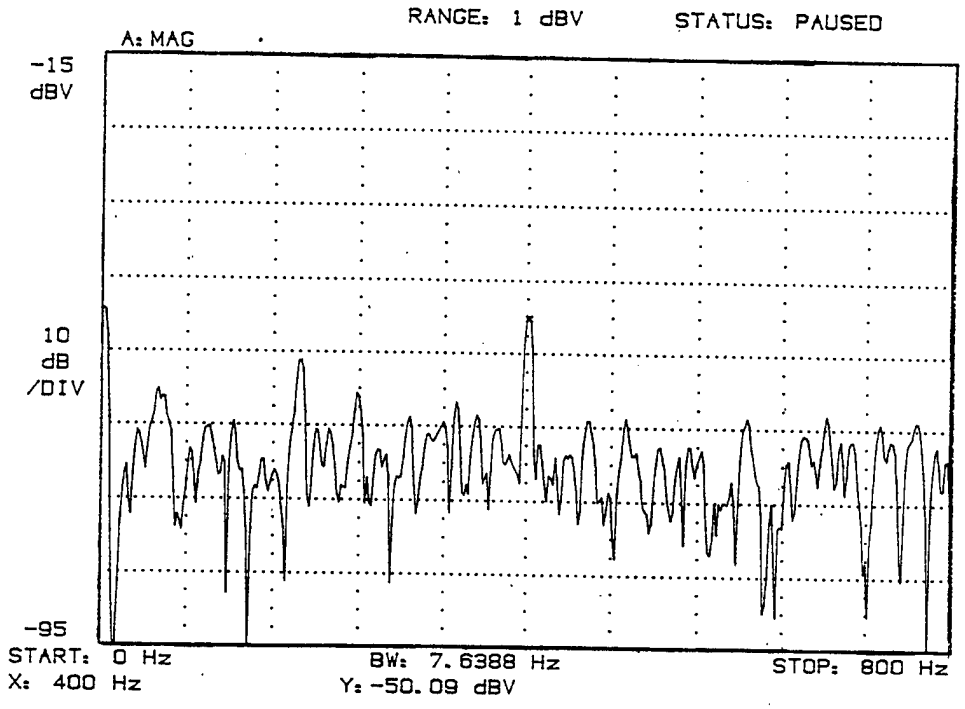

Figure 4-1. Signal Analyzer Display of 400 Hz Target Vibrational Frequency with no Averaging . X is the Horizontal Axis in Hz and Y is the Vertical Axis in dBV.

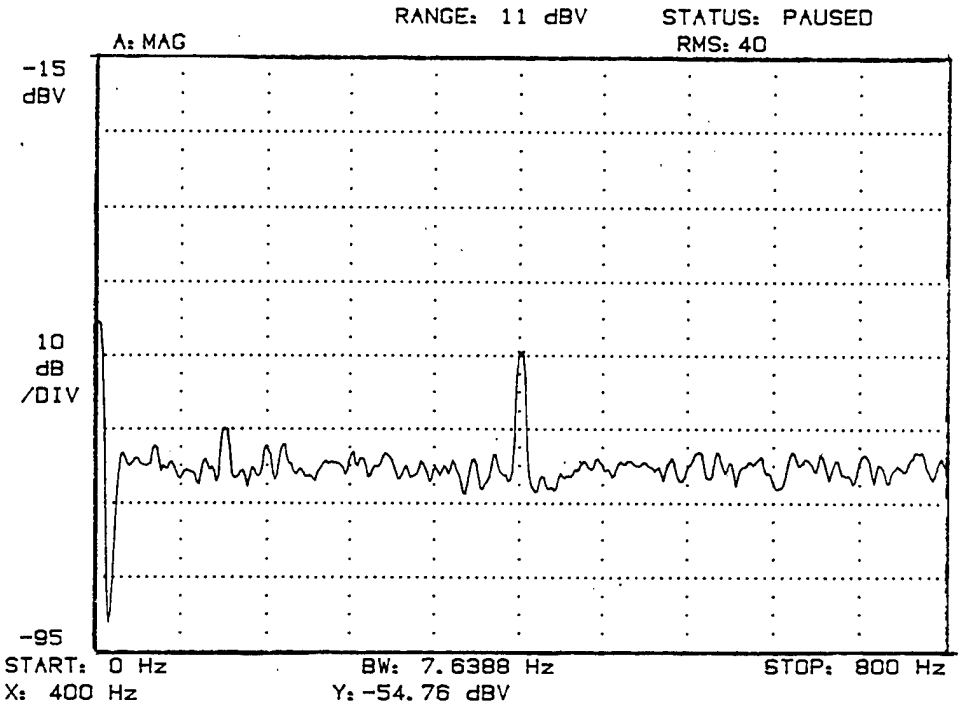

Figure 4-2. Signal Analyzer Display of 400 Hz Target Vibrational Frequency. X is the Horizontal Axis in Hz and Y is the Vertical Axis in dBV. Number of Averages: 40.

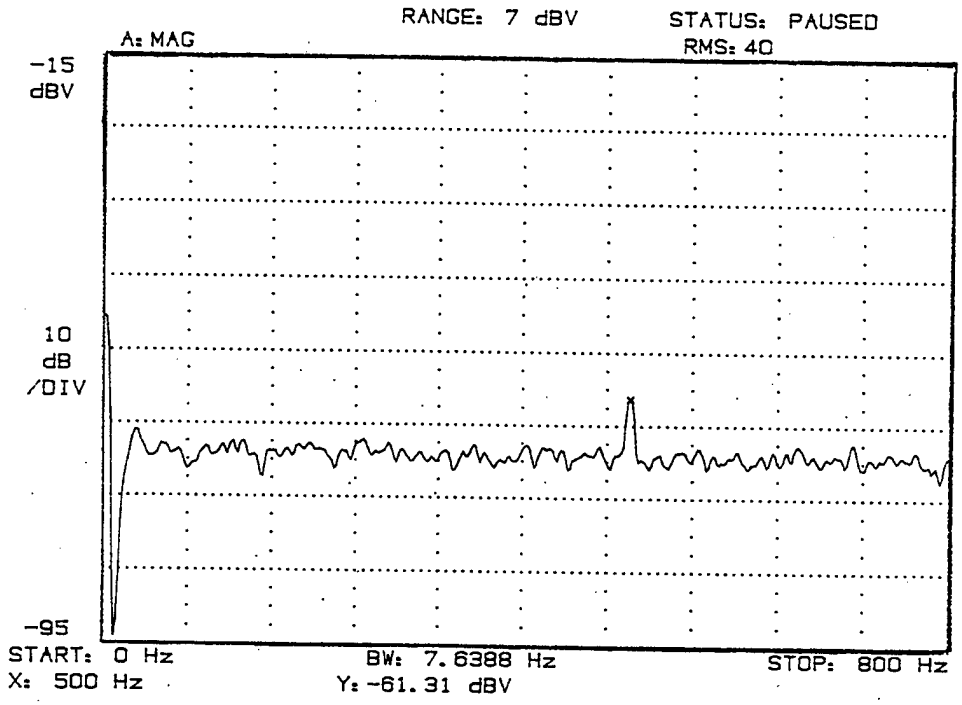

Figure 4-3. Signal Analyzer Display of 500 Hz Target Vibrational Frequency. X is the Horizontal Axis in Hz and Y is the Vertical Axis in dBV. Number of Averages: 40.

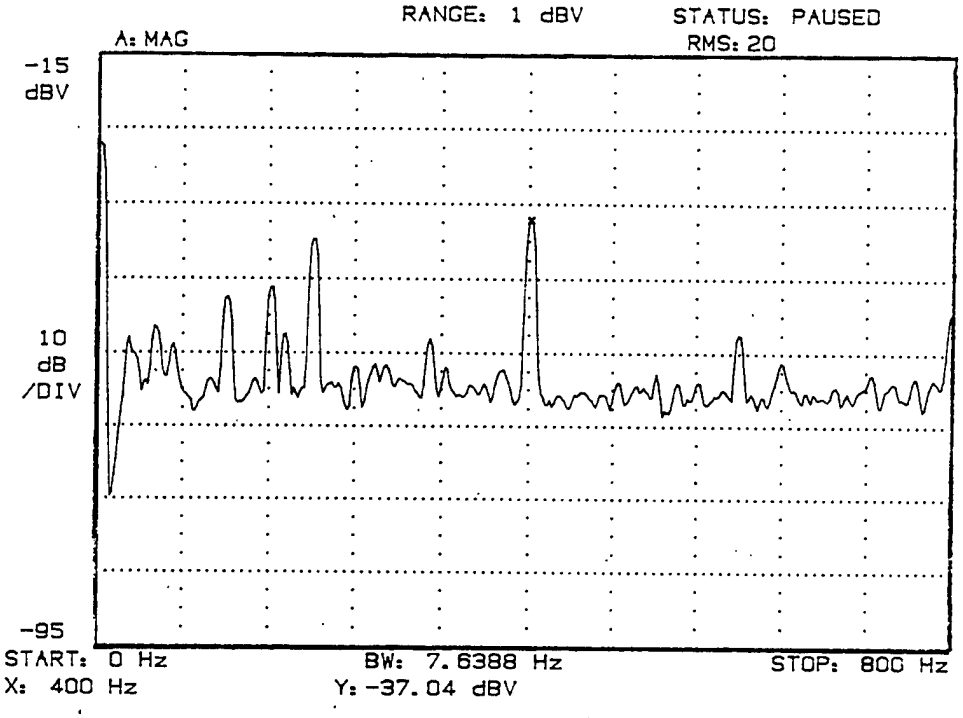

Figure 4-4. Signal Analyzer Display of 400 Hz Target Vibrational Frequency during Fluctuations and also Signal Analyzer Display of Unwanted Frequencies of 120 Hz, 160 Hz, and 200 Hz. X is the Horizontal Axis in Hz and Y is the Vertical Axis in dBV. Number of Averages: 20.

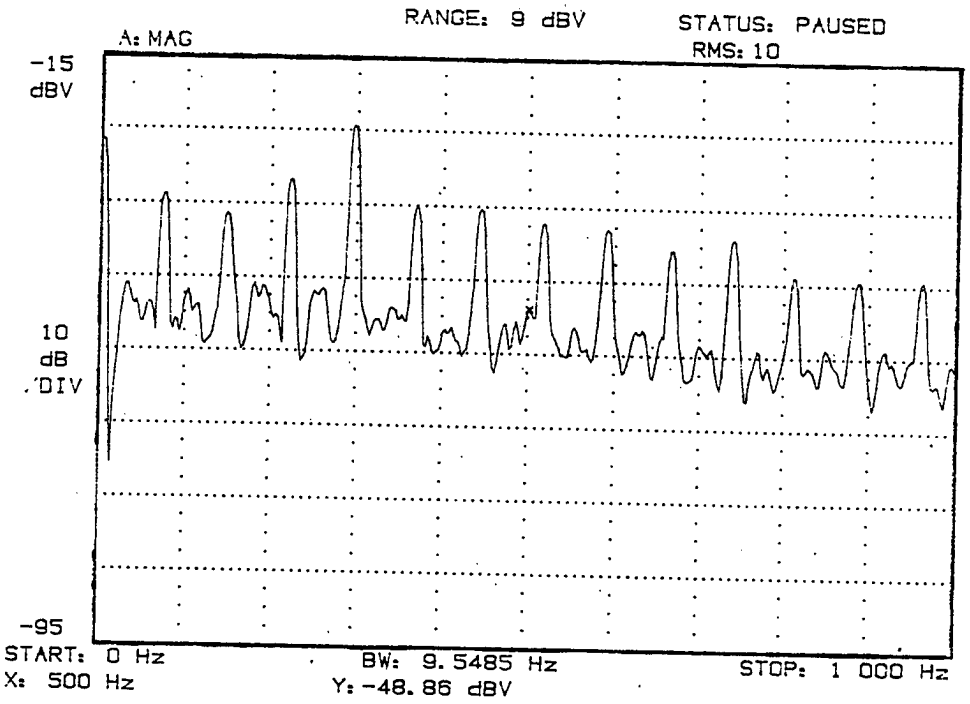

Figure 4-5. Signal Analyzer Display of DC Motor Frequency Spectrum for 1000 Hz Frequency Span and DC Motor Supplied Voltage of 10 volts. X is the Horizontal Axis in Hz and Y is the Vertical Axis in dBV. Number of Averages: 10.

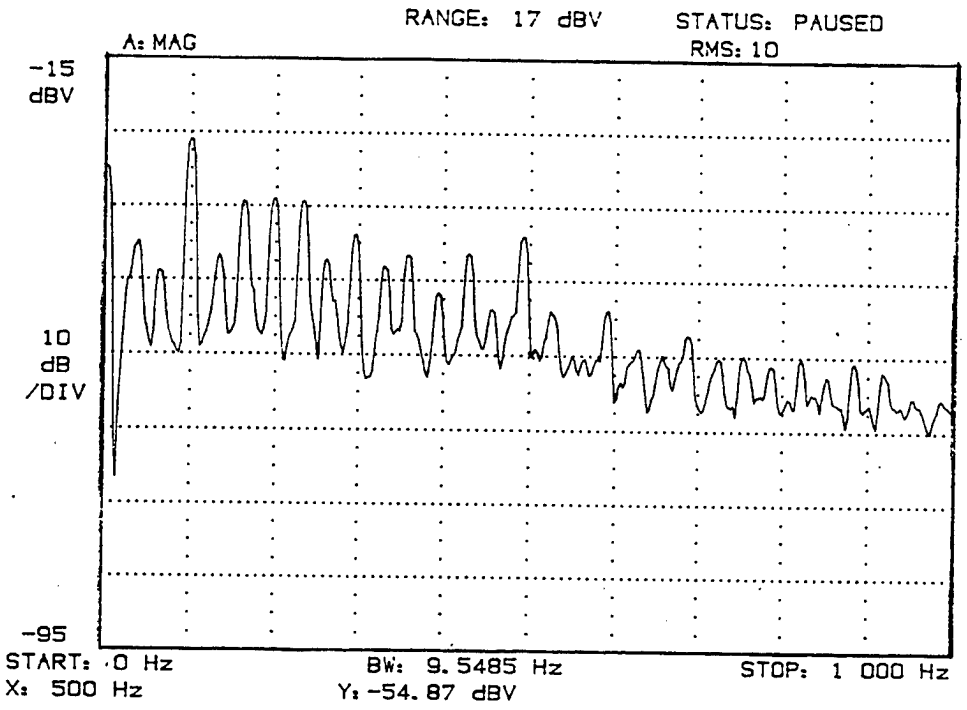

Figure 4-6. Signal Analyzer Display of DC Motor Frequency Spectrum for 1000 Hz Frequency Span and DC Motor Supplied Voltage of 13 volts. X is the Horizontal Axis in Hz and Y is the Vertical Axis in dBV. Number of Averages: 10.

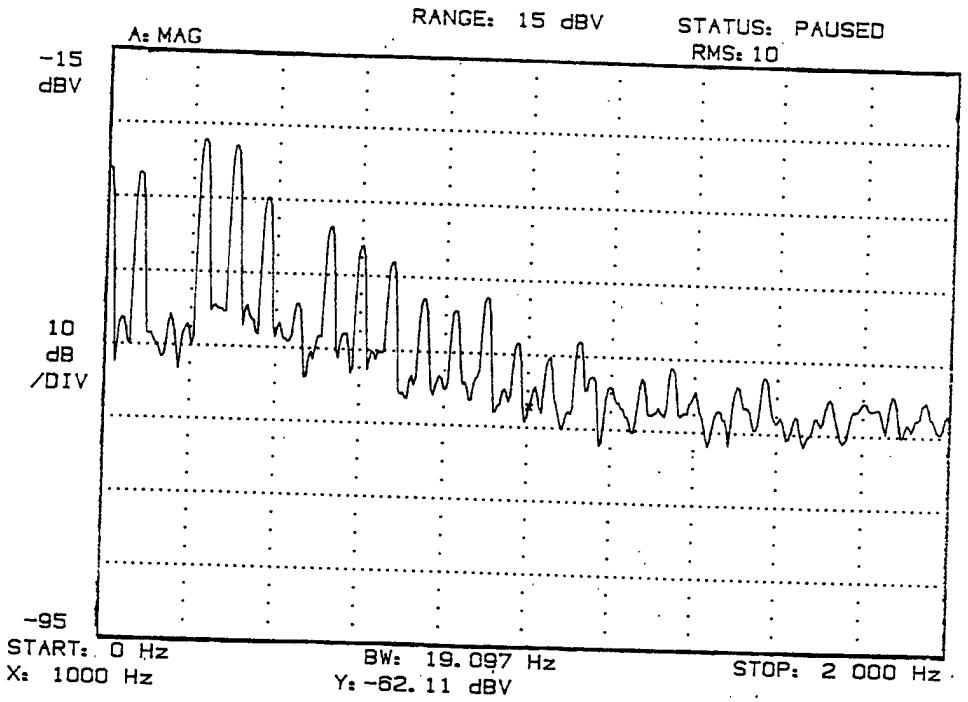

Figure 4-7. Signal Analyzer Display of DC Motor Frequency Spectrum for 2000 Hz Frequency Span and DC Motor Supplied Voltage of 10 volts. X is the Horizontal Axis in Hz and Y is the Vertical Axis in dBV. Number of Averages: 10.

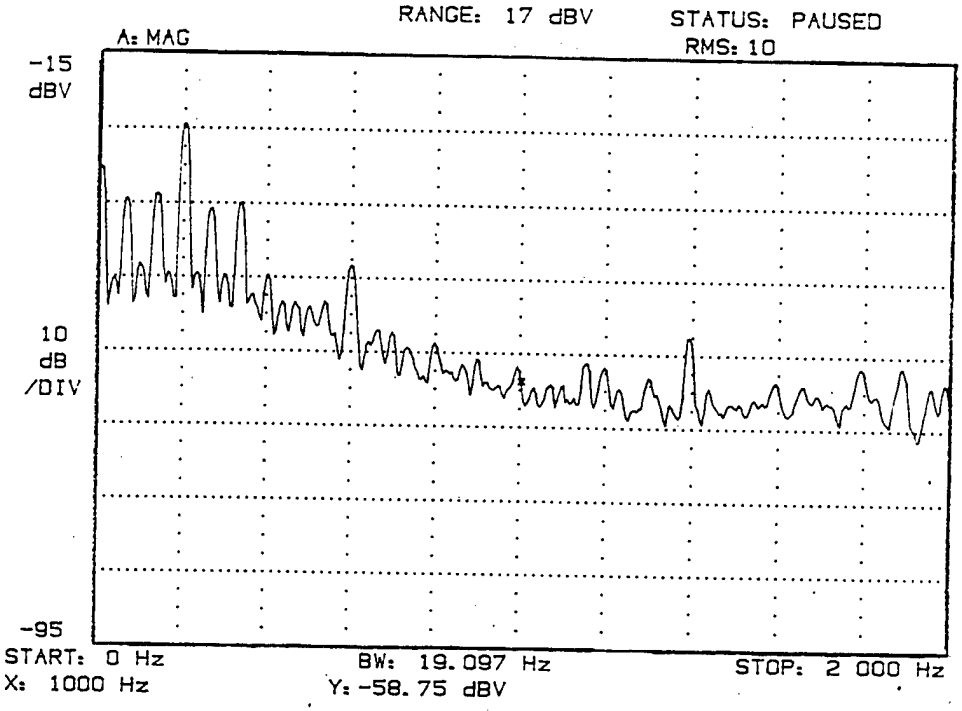

Figure 4-8. Signal Analyzer Display of DC Motor Frequency Spectrum for 2000 Hz Frequency Span and DC Motor Supplied Voltage of 13 volts. X is the Horizontal Axis in Hz and Y is the Vertical Axis in dBV. Number of Averages: 10.

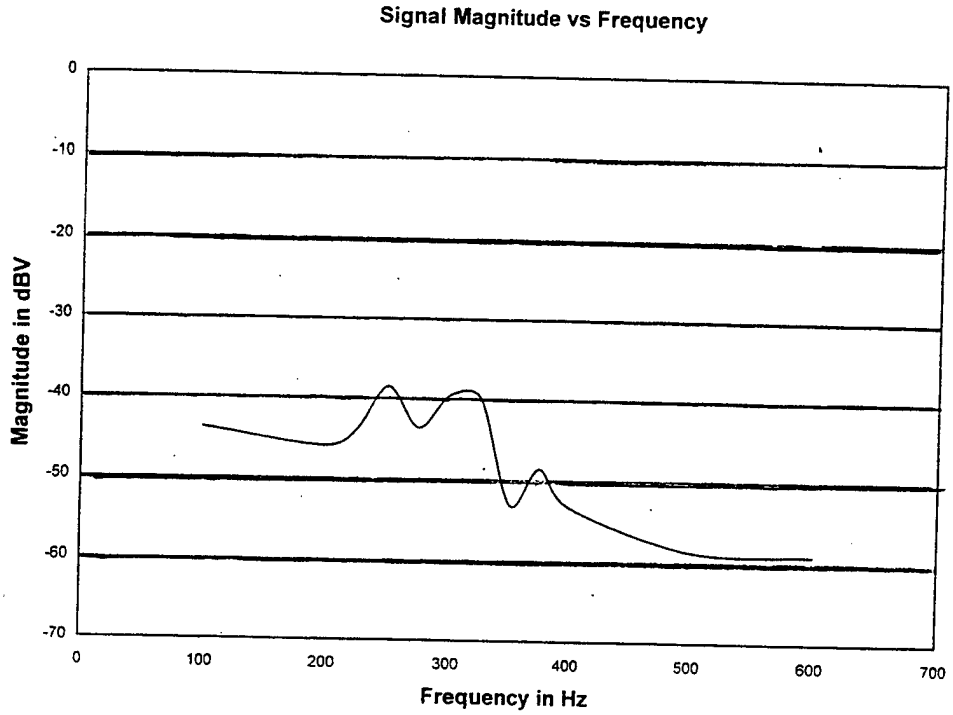

Figure 4-9. Target Sinusoidal Vibration Transfer Function of the Retro-Reflector and Piezoelectric Actuator for a Fixed Sinusoidal Voltage of 18 volts vs Frequency.

LIST OF REFERENCES

Day, James V., *Construction of a Continuous Wave Frequency Modulated Laser Radar for Use in Target Identification,* Naval Postgraduate School Thesis, Monterey, California, 1997.

Harney, Robert C., *Laser Radar Systems: Theory, Technology, and Applications,* Lectures Notes, Monterey, California, 1993.

Hecht, Eugene, *Optics, 2nd Edition,* Addison-Wesley Publishing Company, Inc., 1987.

Sanders, James V., Coppens, Alan B., Frey, Austin R., and Kinsler, Lawrence E., *Fundamentals of Acoustics, 3rd Edition*, John Wiley & Sons, New York, 1982.

Wilson, J. and Hawkes, J. F. B., *Optoelectronics, an Introduction, 2nd Edition,* Prentice Hall, New York, New York, 1989.

INITIAL DISTRIBUTION LIST

1. Defense Technical Information Center..... 2
   8725 John J. Kingman Rd., STE 0944
   Ft. Belvoir, Virginia 22060-6218

2. Library, Code..... 2
   Naval Postgraduate School
   411 Dyer Rd.
   Monterey, California 93943-5101

3. Professor Robert C. Harney (Code PH/Ha)..... 1
   Naval Postgraduate School
   Monterey, CA 93943

4. Professor Donald L. Walters (Code PH/ WE)..... 1
   Naval Postgraduate School
   Monterey, CA 93943

5. Chairman (Code PH)..... 1
   Department of Physics
   Naval Postgraduate School
   Monterey, CA 93943

6. Pierre Hilaire..... 1
   4405 Pembridge Avenue
   Orlando, FL 32826